molecules

MDPI

Article

Multitargeting Histamine H_3 Receptor Ligands among Acetyl- and Propionyl-Phenoxyalkyl Derivatives

Dorota Łażewska [1,*], Maria Kaleta [1], Paula Zaręba [2], Justyna Godyń [2], Mariam Dubiel [3], Ewelina Honkisz-Orzechowska [1], Agata Doroz-Płonka [1], Anna Więckowska [2], Holger Stark [3] and Katarzyna Kieć-Kononowicz [1]

[1] Department of Technology and Biotechnology of Drugs, Faculty of Pharmacy, Jagiellonian University Medical College in Kraków, Medyczna 9, 30-688 Kraków, Poland
[2] Department of Physicochemical Drug Analysis, Jagiellonian University Medical College in Kraków, Medyczna 9, 30-688 Kraków, Poland
[3] Institute of Pharmaceutical and Medicinal Chemistry, Heinrich Heine University Düsseldorf, Universitaetsstr. 1, 40225 Düuesseldorf, Germany
* Correspondence: dorota.lazewska@uj.edu.pl

Abstract: Alzheimer's disease (AD) is a neurodegenerative disorder, for which there is no effective cure. Current drugs only slow down the course of the disease, and, therefore, there is an urgent need to find effective therapies that not only treat, but also prevent it. Acetylcholinesterase inhibitors (AChEIs), among others, have been used for years to treat AD. Histamine H_3 receptors (H_3Rs) antagonists/inverse agonists are indicated for CNS diseases. Combining AChEIs with H_3R antagonism in one structure could bring a beneficial therapeutic effect. The aim of this study was to find new multitargetting ligands. Thus, continuing our previous research, acetyl- and propionyl-phenoxy-pentyl(-hexyl) derivatives were designed. These compounds were tested for their affinity to human H_3Rs, as well as their ability to inhibit cholinesterases (acetyl- and butyrylcholinesterases) and, additionally, human monoamine oxidase B (MAO B). Furthermore, for the selected active compounds, their toxicity towards HepG2 or SH-SY5Y cells was evaluated. The results showed that compounds **16** (1-(4-((5-(azepan-1-yl)pentyl)oxy)phenyl)propan-1-one) and **17** (1-(4-((6-(azepan-1-yl)hexyl)oxy)phenyl)propan-1-one) are the most promising, with a high affinity for human H_3Rs (K_i: 30 nM and 42 nM, respectively), a good ability to inhibit cholinesterases (**16**: AChE IC_{50} = 3.60 μM, BuChE IC_{50} = 0.55 μM; **17**: AChE IC_{50} = 1.06 μM, BuChE IC_{50} = 2.86 μM), and lack of cell toxicity up to 50 μM.

Keywords: histamine H_3 receptor ligand; cholinesterase inhibitor; kinetic studies; toxicity; HepG2 lines; SH-SY5Y lines

check for updates

Citation: Łażewska, D.; Kaleta, M.; Zaręba, P.; Godyń, J.; Dubiel, M.; Honkisz-Orzechowska, E.; Doroz-Płonka, A.; Więckowska, A.; Stark, H.; Kieć-Kononowicz, K. Multitargeting Histamine H_3 Receptor Ligands among Acetyl- and Propionyl-Phenoxyalkyl Derivatives. *Molecules* **2023**, *28*, 2349. https://doi.org/10.3390/molecules28052349

Academic Editor: Rosa Amoroso

Received: 13 January 2023
Revised: 13 February 2023
Accepted: 28 February 2023
Published: 3 March 2023

Copyright: © 2023 by the authors. Licensee MDPI, Basel, Switzerland. This article is an open access article distributed under the terms and conditions of the Creative Commons Attribution (CC BY) license (https://creativecommons.org/licenses/by/4.0/).

1. Introduction

The pathological cause of Alzheimer's disease (AD) is neuronal death, which leads to the disruption of connections between neurons and the inhibition of the processing and conduction of electrical impulses. This is caused by the accumulation of protein deposits in neuronal tissue: ß-amyloid or tau protein [1,2]. Recently, it has been indicated that α-synuclein may also play an important role in the pathogenesis of AD [3]. Presumably, there is a feedback loop between all these proteins. β-Amyloid increases GSK-β kinase levels, which induces tau protein phosphorylation and stimulates α-synuclein production. All of this can lead to the aggregation of both the β-amyloid and the tau protein. However, as AD is a disease with a complex a etiology, in addition to the factors discussed above, many more play a role in its development and course [1]. Among these, impaired cholinergic transmission is discussed as an important contributor.

The theory of the involvement of acetylcholine (ACh) in the development of AD has been known since the 1970s [4], and is based on the observation of reduced levels of this

neurotransmitter in the brains of AD patients, leading to problems with cognition and memory. Cholinesterases (acetyl- and butyrylcholinesterase), especially acetylcholinesterase (AChE), play important roles in the degradation of ACh, which, under normal conditions, ensures the proper transmission of neuronal signals. Under pathological conditions, when these enzymes are overexpressed, ACh can be over-degraded, and many factors important in the development of AD may be affected (e.g., β-amyloid formation, tau protein phosphorylation, or neuroinflammation) [5]. One possible way to increase ACh levels is to reduce the activity of these enzymes by using their inhibitors. In the 1990s, the first AChE inhibitors were introduced to therapy (tacrine-1993 and donepezil-1996), followed by others in the following years (rivastigmine-2000 and galantamine 2001), and are used (except tacrine, which was withdrawn in 2013) as key drugs in the treatment of AD [6].

Since then, the search for other active AChE inhibitors has been ongoing, and many compounds based on the structures of known inhibitors or structurally new compounds have been described in the literature [7]. Recently, the interest has focused on the search for multitarget ligands, as it is believed that such compounds may be more effective in the treatment of diseases with multiple etiologies, including AD [8]. Among these compounds, ligands are described that act simultaneously on AChE and histamine H_3 receptors (H_3R) [9]. H_3Rs were first described in the 1980s by Arrang et al. [10]. They are mainly located presynaptically in neurons of the central nervous system (CNS), especially in regions associated with memory, cognition, and arousal [11,12]. H_3Rs influence the level of histamine itself and affect the release of other neurotransmitters, including ACh. The blocking of H_3Rs increases neurotransmitter release. Many preclinical studies suggest the utility of H_3R antagonists/inverse agonists in different CNS diseases, including AD [13,14]. Although clinical studies with H_3R ligands did not show higher benefits than the currently used AChE inhibitors, it is believed that multitarget compounds combining these two activities may have more positive effects [15]. Quite recently, a crystal structure of human H_3R (hH_3R) in a complex with PF-03654746 (H_3R ligand) was described [16] showing the conservative mode of ligand interactions and hydrophobic contacts in the bottom part of the binding pocket. This finding may be very helpful in the search for new potent compounds.

In recent years, many interesting papers have been published, describing multitarget H_3R ligands with potential use in AD therapy [17–22]. The structures of the most promising H_3R compounds with cholinesterase inhibition activities in the last three years are shown in Figure 1. Some of them, such as compounds **IV** and **V** (Figure 1), showed inhibitory activity targeting monoamine oxidase B (MAO B). MAO B inhibitors are known to increase the level of dopamine (DA) in the brain, stopping its metabolism and reducing reactive oxygen species produced during this metabolism [23]. Moreover, the latest studies show that DA levels are reduced in AD patients [24]. Furthermore, it is thought that DA may also play an important role in the pathogenesis of AD [25].

The aim of this study was to synthesize and pharmacologically test acetyl- and propionylphenoxyalkyl derivatives designed, on the basis of our previous work, as H_3R ligands and cholinesterase inhibitors [20,26]. The compounds obtained were tested in in vitro assays to estimate their pharmacological activity (H_3Rs, AChE, BuChE, MAO B). Moreover, selected compounds were evaluated for any toxic effects on HepG2 and SH-SY5Y cell lines.

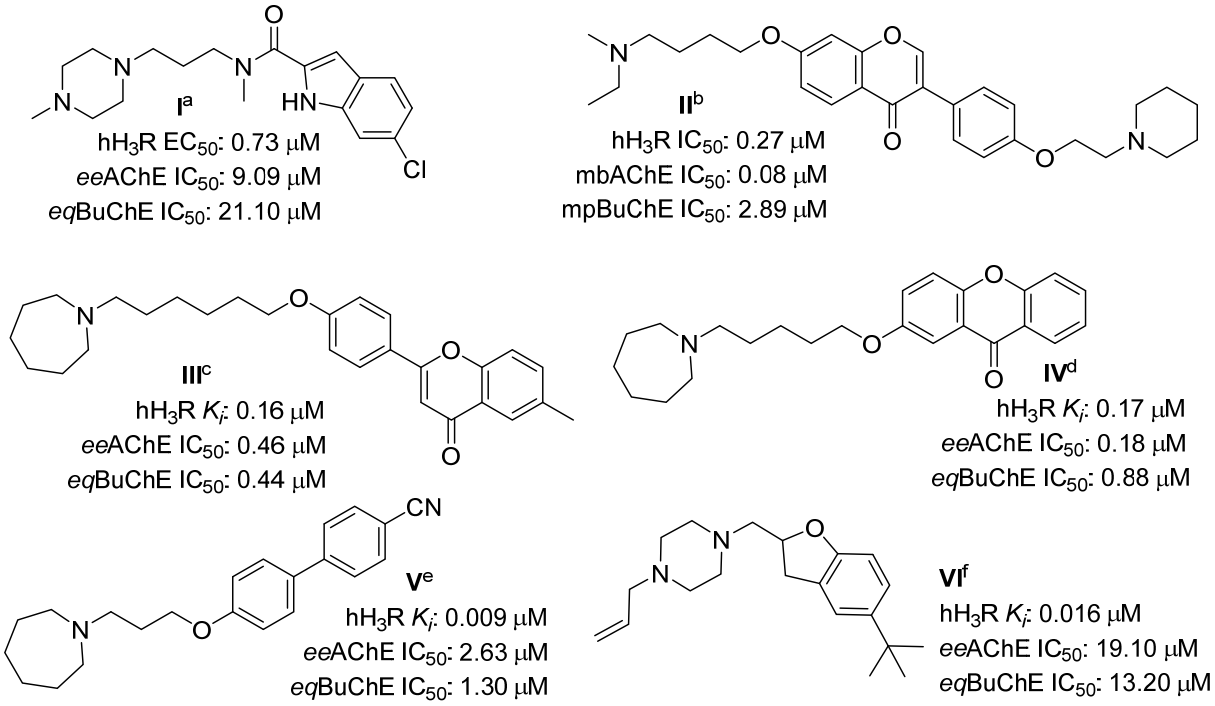

Figure 1. Structures of the most promising histamine H_3R ligands with cholinesterase inhibitory activity from the last 3 years. hH_3R—human H_3R; *ee*AChE—AChE from electric eel; *eq*BuChE—BuChE from equine serum; mbAChE—AChE extracted from mouse brains; mpAChE—AChE extracted from mouse plasma. [a] Data from [17]; [b] data from [18]; [c] data from [19]; [d] data from [20]; [e] data from [21]; [f] data from [22].

2. Results

2.1. Design of Compounds

Three years ago, through in silico studies (molecular modeling and docking to cholinesterases), xanthones were found to be potential ligands for H_3R, cholinesterases and MAO B [20]. The designed compounds aligned with the general construction pattern of previously suggested H_3R antagonists/inverse agonists (Figure 2) [27].

Then, xanthones were synthesized, and tested in vitro, in appropriate assays that confirmed their biological activity against these targets, which have been previously described by Łażewska et al. [20]. The most promising structure found in that work, compound **IV** (Figure 1), was selected as the **lead 1** for further modifications, in order to check which fragments of the xanthone moiety affect their pharmacological activity. As a first step, oxygen was removed from this molecule to obtain benzophenone derivatives that have recently been described [26]. The direction of the modifications is shown in Figure 3. Among the benzophenone derivatives, there were structures that showed good activity as multitarget ligands (e.g., the structures in Figure 3). The aim of the current work was to test whether further structural modifications (reduction of substituent size), i.e., replacing the phenyl moiety with an ethyl or a methyl group, would improve or worsen interactions with selected biological targets. In the search for CNS-active compounds (but not exclusively), it is important that compounds have moderate lipophilicity (log P in the range of one to three), as this favorably affects ADMET parameters and increases the compound's chances of being a drug [28]. Replacing the phenyl ring with an alkyl (methyl, ethyl) substituent provides a reduction in the lipophilicity of the compounds, which was confirmed by preliminary calculations performed using the SwissADME server [29] (data in Supplementary Materials).

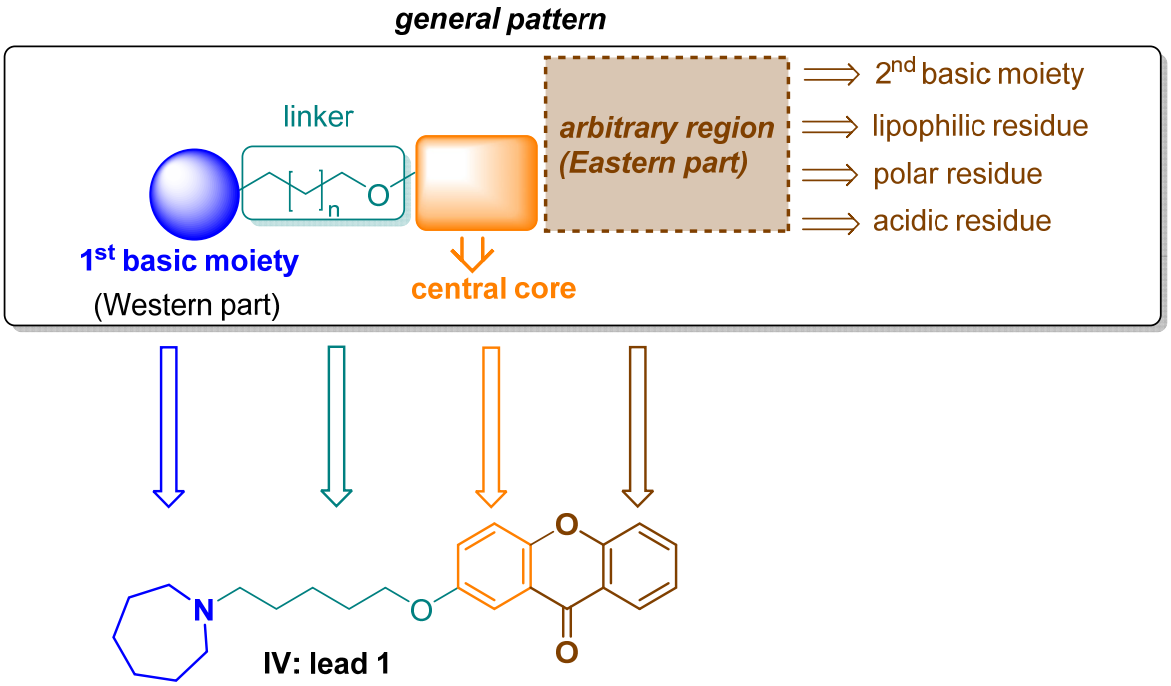

Figure 2. Pharmacophore model of H_3R antagonists/inverse agonists and the **lead 1**.

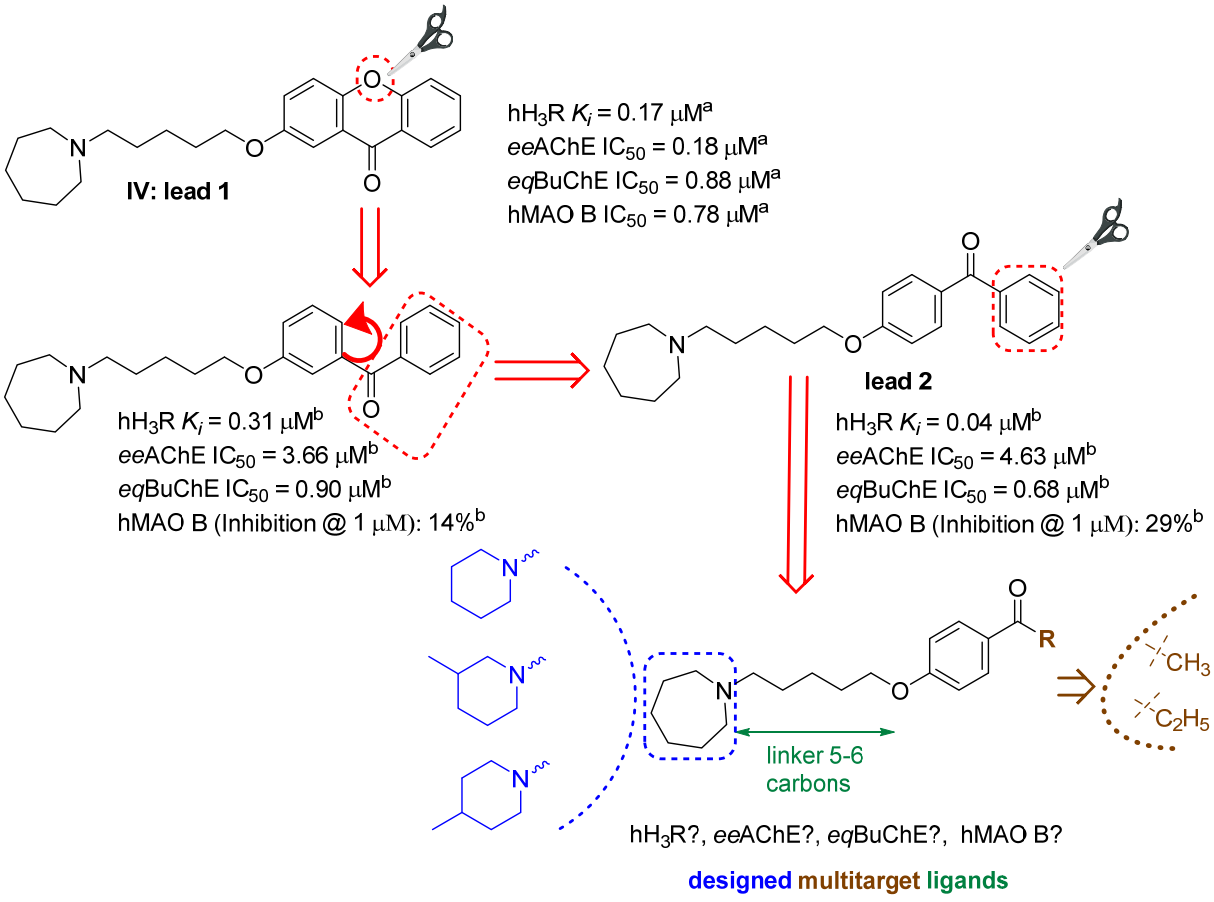

Figure 3. Lead compounds and modification strategies. [a] Data from [20]; [b] data from [26].

2.2. Synthesis of Compounds **2**–**17**

In the first stage, it was necessary to obtain phenoxyalkylbromides (**1a**–**1d**; Scheme 1) by *O*-alkylation of the corresponding phenols with 1,5-dibromopentane or 1,6-dibromohexane. The reactions were performed in freshly prepared sodium propanolate. The resulting bromides were then subjected to *N*-alkylation with the corresponding amines (piperidines or azepane; Scheme 1). The reactions were carried out in the mixture of ethanol and water (21:4), in the presence of potassium carbonate and catalytic amounts of potassium iodide. The final products were purified by extraction. The oily free bases were transformed into oxalic acid salts. The purity and identity of the products were confirmed by spectroscopic methods (^{1}H and ^{13}C NMR, LC-MS) and elemental analysis. Spectra data are presented in the Supplementary Materials.

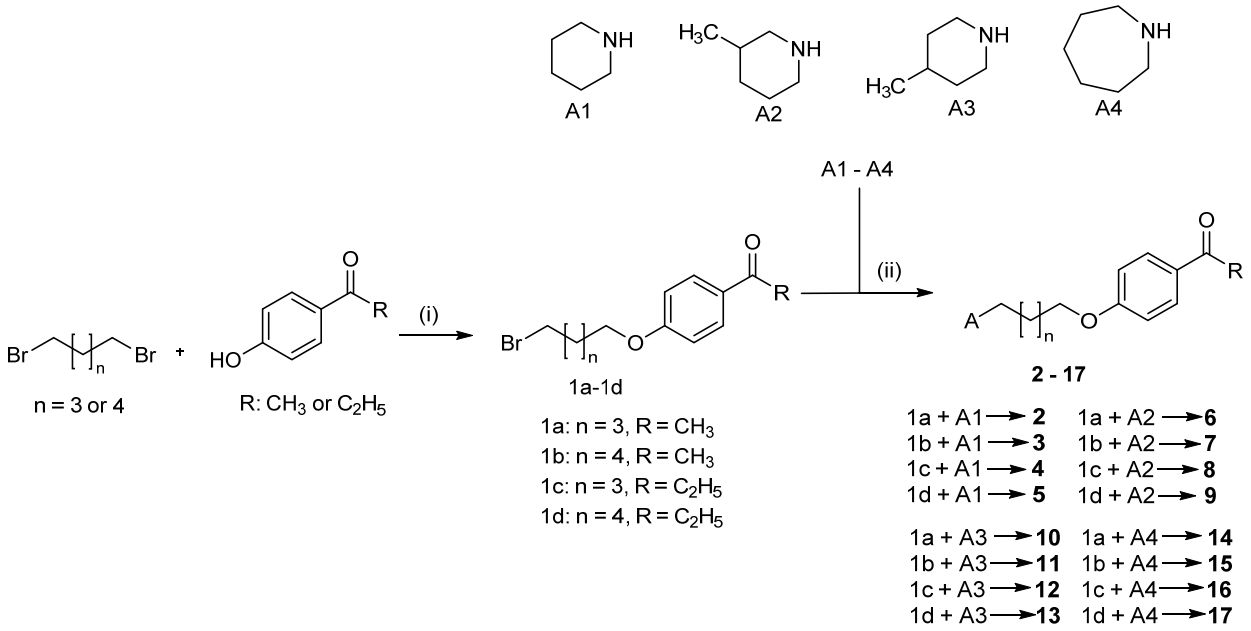

Scheme 1. Synthesis of the designed compounds **2**–**17**. Reagents and conditions: (i) Na, 1-propanol, 3 h—60 °C, 3 h—reflux; (ii) K_2CO_3, KI, ethanol–water (volume ratio 21:4). Yield: 28–48%.

2.3. Human Histamine H_3 Receptor Affinity

The affinity for hH_3R was assessed in vitro in radioligand binding assays, using membrane preparations of HEK293 cells stably expressing hH_3R, while [^{3}H]-N^{α}-methylhistamine was used as a radioligand. The exact procedure was described previously by Kottke et al. [30]. Novel compounds were tested as oxalic acid salts. All compounds (except for **9** and **10**) showed very good affinities for these receptors, with K_i values below 100 nM (Table 1). The activity depended on all three variables, i.e., the presence of an amine group, the chain length (five or six carbons), and the type of substituent in the phenyl ring. With regard to the change in the amine moiety, it can be observed that, regardless of the length of the chain and the type of R substituent, the activity of the derivatives was arranged in the following order: 3-methylpiperidine ≥ piperidine ≥ azepane >> 4-metylpiperidine derivatives. Regarding the length of the carbon chain, compounds bearing the pentylene chain are characterized by a higher binding affinity to the receptor than hexylene derivatives (exception: **10**). The change of the acyl group to propionyl one resulted in an almost twofold increase in affinity to hH_3R receptors (exception **4**). The highest affinity for hH_3R among all compounds was observed in compound **8**, with a K_i of 12 nM. Seven other compounds (**2**, **4**, **5**, **6**, **9**, **16** and **17**) had also very high affinities, with K_i values < 50 nM.

Table 1. Histamine H_3 receptor affinities, cholinesterases, and MAO B inhibitory activity of the tested compounds.

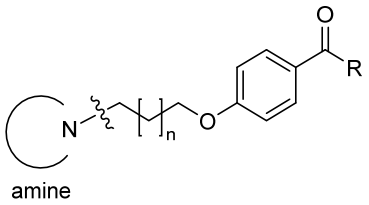

Comp	Amine	n	R	hH_3R [a] K_i (nM) Mean [CI 95%]	*ee*AChE [b] IC_{50} (μM) Mean ± SEM (% inh) [e]	*eq*BuChE [c] IC_{50} (μM) Mean ± SEM (% inh) [e]	hMAO B [d] (% inh) [f]
2	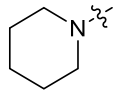	3	CH_3	34 [24;47]	(45%)	(25%)	(2%)
3		4	CH_3	75 [34;169]	(67%)	(23%)	(3%)
4		3	C_2H_5	24 [11;54]	(49%)	(32%)	(16%)
5		4	C_2H_5	41 [27;64]	4.79 ± 0.19	1.35 ± 0.04	(22%)
6	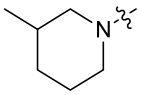	3	CH_3	26 [13;52]	3.06 ± 0.10	(14%)	(10%)
7		4	CH_3	72 [41;127]	1.75 ± 0.05	(18%)	(0%)
8		3	C_2H_5	12 [6;22]	2.10 ± 0.06	1.75 ± 0.05	(19%)
9		4	C_2H_5	38 [20;72]	(68%)	(66%)	(12%)
10	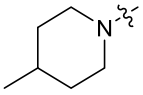	3	CH_3	120 [82;177]	(60%)	(43%)	(0%)
11		4	CH_3	106 [76;149]	2.65 ± 0.11	(49%)	(0%)
12		3	C_2H_5	57 [36;91]	(58%)	1.29 ± 0.08	(0%)
13		4	C_2H_5	58 [35;96]	2.56 ± 0.08	(65%)	(1%)
14	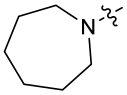	3	CH_3	52 [38;71]	(63%)	(63%)	(37%)
15		4	CH_3	79 [41;150]	(67%)	(68%)	(6%)
16		3	C_2H_5	30 [17;53]	3.60 ± 0.12	0.55 ± 0.02	(6%)
17		4	C_2H_5	42 [20;85]	1.06 ± 0.03	2.86 ± 0.03	(5%)
pitolisant				12 ± 3 [g]	(3%) [g]	8.42 ± 0.18 [g]	(2%) [g]
donepezil				nt [h]	0.04 ± 0.01 [g]	1.83 ± 0.02	nt [h]
safinamide				nt [h]	nt [h]	nt [h]	(98%) 7.60 ± 1.0 [i]

[a] [^{3}H]-N^{α}-Methylhistamine binding assay performed in HEK293 cells expressing the human H_3 receptor; mean value with a confidence interval (CI95%) from at least three independent repetitions [b] AChE of *electric eel*; IC_{50}, mean value of three independent experiments; [c] BuChE of *equine serum*; IC_{50}, mean value of three independent experiments. [d] Fluorometric Amplex™ red MAO assay. [e] Percentage inhibition of *ee*AChE or *eq*BuChE at 10 μM. [f] Percentage inhibition of hMAO B at 1 μM; mean values of two independent experiments. [g] Data from Ref. [19]. [h] Not tested. [i] IC_{50} in nM; data from ref. [20].

2.4. Cholinesterase Inhibitory Activity

All compounds were tested at a concentration of 10 μM in a modified colorimetric method first described by Ellman et al. in the 1960s [19,31], using AChE from *electrophorus electricus* (*ee*AChE) and BuChE from *equine serum* (*eq*BuChE). The compounds (**5**–**8**, **11**–**13**, **16** and **17**) that showed inhibitions of greater than 70% were selected for further studies, in order to obtain IC_{50} values. All results are collected in Table 1. The IC_{50} values are in the low micromolar range (<5 μM). In general, compounds that showed activity against both cholinoesterases inhibited BuChE to a greater extent than AChE (with the exception of **17**). However, we did not observe any difference in inhibition potency. No correlation was observed between inhibitory activity and hH_3R affinity. The most interesting compounds were among the azepane derivatives. Compound **16** is the most potent BuChE inhibitor in the whole series, with inhibitory activity in the sub-micromolar range (IC_{50} = 0.55 μM). In contrast, compound **17** shows the highest inhibition of AChE in this series, with a potency of one micromole (IC_{50} = 1.06 μM).

Kinetic Studies of the Inhibition of *ee*AChE and *eq*BuChE

For the most active compounds, **17** (AChE inhibitor) and **16** (BuChE inhibitor), tests were carried out to determine the type of inhibition exhibited for the appropriate enzymes. The Michaelis–Menten equation was used to calculate the maximum velocity (V_{max}) and the Michaelis constant (K_m).

Lineweaver–Burk plots obtained for **17** (Figure 4A) showed a series of lines converging at the same point near the x-axis (1/[ATC], which confirmed the non-competitive (mixed) type of *ee*AChE inhibition, as V_{max} decreased with increasing concentrations of inhibitor.

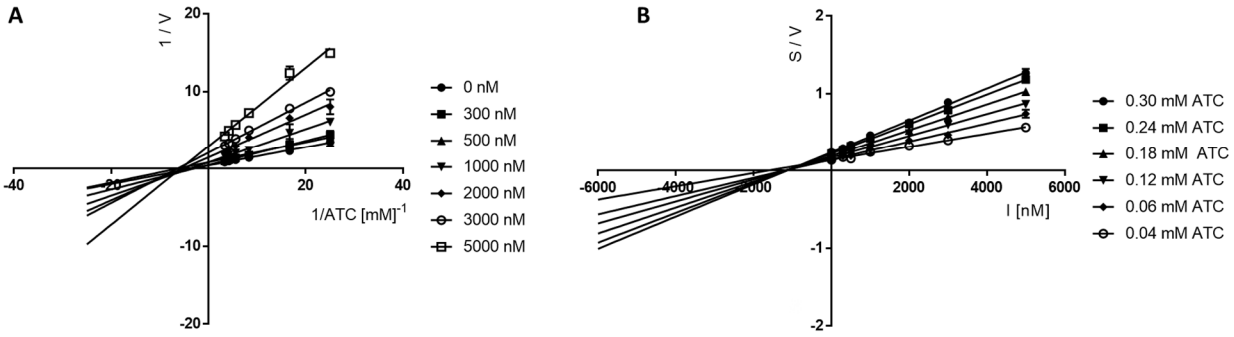

Figure 4. Lineweaver−Burk (**A**) and Cornish−Bowden (**B**) plots illustrating mixed types of *ee*AChE inhibition by compound **17**. S = acetylthiocholine; V = initial velocity rate; I = inhibitor concentration.

Furthermore, Cornish–Bowden plots (S/V vs. I) obtained for **17** (Figure 4B) showed a series of lines converging at the same point over the x-axis, thus confirming a mixed mechanism of cholinesterase inhibition. The same situation was observed for compound **16,** for which the type of BuChE inhibition was investigated and evaluated in the Lineweaver–Burk and Cornish–Bowden plots (Figure 5). The type of line intersection and the location of this intersection confirms the mixed type of inhibition.

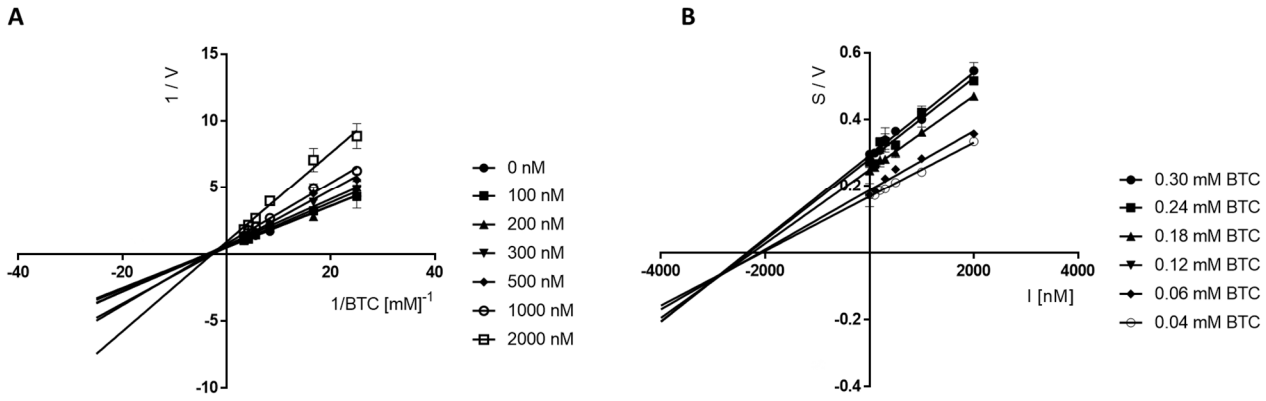

Figure 5. Lineweaver−Burk (**A**) and Cornish−Bowden (**B**) plots illustrating mixed types of *eq*BuChE inhibition by compound **16**. S = butyrylthiocholine; V = initial velocity rate; I = inhibitor concentration.

2.5. Monoamine Oxidase B Inhibitory Activity

The ability to inhibit MAO B was estimated by a fluorescence assay, as previously described [32]. The screening assay was carried out at a concentration of 1 μM to determine the percentage inhibition of the enzyme, as compared to reference inhibitors (i.e., pargiline, rasagiline and safinamide). All compounds showed weak percentage of inhibition (<50%) and were not selected for further testing (Table 1).

2.6. Cytotoxicity Studies of Selected Compounds

Compounds showing activity against cholinesterases (AChE and/or BuChE) were selected for preliminary evaluation of their toxic effects (i.e., compounds **5**–**8**, **11**–**13**, **16** and

17) in the MTS assay. The studies were conducted on two cell lines: HepG2 and SH-SY5Y. To assess viability, increasing concentrations of the compounds tested (from 0.78 μM to 50 μM) were incubated with their respective cell lines (HepG2 or SH-SY5Y) for 48 h and 24 h, respectively. After the indicated time, the MTS reagent was added directly to the cultured cells for 1 h, and then the absorbance at 490 nm was read. The study showed that both the tested lines (HepG2 and SH-SY5Y) remained more than 50% viable the highest doses tested. The results are presented in Table 2 and Figures S1 and S2 (Supplementary Materials).

Table 2. Summary of toxicity evaluation of selected compounds in MTS assay.

Compound	HepG2 [a] IC_{50} [μM]	Cell Viability (%) [b]	SH-SY5Y [a] IC_{50} [μM]	Cell Viability (%) [b]
5	158	69.55 ± 2.14	-	No toxic effect
6	120	74.32 ± 5.58	149	86.23 ± 2.20
7	148	72.38 ± 4.54	-	No toxic effect
8	142	70.89 ± 2.92	349	90.73 ± 1.50
11	223	77.52 ± 0.94	-	No toxic effect
12	149	77.20 ± 4.14	421	90.70 ± 12.88
13	105	64.66 ± 4.40	-	No toxic effect
16	92	67.69 ± 1.14	357	90.28 ± 5.32
17	60	58.02 ± 3.54	111	70.35 ± 4.46

[a] The IC_{50} value from the MTS assay in HepG2 and SH-SY5Y cells, at 48 h and 24 h of exposure, respectively. IC_{50} values were calculated with a non-linear regression fit to a sigmoidal dose–response curve (log of compound concentration vs. normalized response) using GraphPad Prism (v. 4.0.3). [b] Cell viability at the concentration of 50 μM, expressed as the percentage of control (vehicle-treated cells), set as 100%.

3. Discussion

Continuing our previous works on searching for multi-targeted H_3R ligands, we obtained a series of sixteen compounds designed on the basis of our previous studies [20,26]. We conducted pharmacological tests of acetyl- and propionyl-phenoxy-pentyl (-hexyl) amines, and confirmed the high affinity of these compounds for hH_3R. The determined K_i values for all compounds are in the nanomolar range (K_i < 120 nM). This is in line with our expectations, as these structures fit the proposed pharmacophore model for H_3R antagonists/reverse agonists [27]. This pharmacophore has the following elements: a basic center, a linker, a central core, and an arbitrary region with high variability, which are required in a molecule for activity. The investigated compounds have all these elements. Among all the used amines (azepane, 3-methylpiperidine, 4-methylpiperidine and piperidine), the least active compounds were the 4-methylpiperidines, and such a correlation was also observed in previous works, e.g., [33]. In regard to the most active compounds, it is difficult to say, without a doubt, as to which amine's presence is most beneficial. The activities of the derivatives with the other three amines are usually comparable, although compounds with a 3-methylpiperidine moiety are often the most active.

As for the results obtained for cholinesterase inhibition, they are also unclear. No clear correlation was observed between the structure of the compounds and the observed inhibitory potency. Only nine of sixteen compounds showed enough activity in the prescreening (>70% at 10 μM) to qualify them for testing at other concentrations to determine the IC_{50} values. All these compounds showed inhibitory potencies in the low micromolar concentration range (0.55 μM ≤ IC_{50} ≤ 4.79 μM). Some of them inhibited, at micromolar concentrations, both cholinesterases (four compounds); others only inhibited one cholinesterase (five compounds), whereas a low percentage of inhibition (<70%) was observed for seven compounds. These results showed, in comparison with recently described benzophenone derivatives [26], that the exchange of the phenyl substituent for an ethyl substituent and, in particular, a methyl substituent, did not favorably influence cholinesterase inhibition. Almost all of the thirty-four previously described benzophenones (with the exception of three compounds) inhibited the cholinesterases in the micromolar range (0.17 μM ≤ IC_{50} ≤ 7.75 μM) [26], while now only nine compounds showed activity against cholinesterases. Comparing the results for the **lead**

2 (Figure 3) directly with analogous compounds **14** (the methyl analogue) and **16** (the ethyl analogue), it was seen that the exchange of the phenyl for the ethyl substituent, in this case, did not affect the activity against all three tested biological targets, i.e., (hH_3R, AChE and BuChE), very significantly. The opposite result was observed for the methyl substituent (**14**). Shortening the chain to the methyl substituent caused a decrease in activity against both cholinesterases (only 63% of inhibition). Among all nine compounds, compound **16** had the highest BuChE inhibitory activity (IC_{50} = 0.55 μM), whereas compound **17** showed the highest inhibition of AChE (IC_{50} = 1.06 μM). Both these compounds had a hexyl carbon linker.

None of the compounds tested showed a promising inhibition of hMAO B.

All compounds that showed inhibitory activity against cholinesterases were selected for further in vitro studies, in order to evaluate potential toxic effects on HepG2 cells and SH-SY5Y cells in the MTS assay. Human liver carcinoma HepG2 cell lines are the most popular lines to assess the risk of hepatotoxicity [34]. The human neuroblastoma SH-SY5Y lines are used in experimental models of AD to assess intracellular factors that lead to AD (e.g., tau-related pathology [35]) or the neuroprotection ability of ligands. The results of these studies showed that the compounds had very low toxicity. Specific IC_{50} values calculated with non-linear regression, and fitted to a sigmoidal dose–response curve, were higher than 90 μM. The only exception was compound **17,** which exhibited some toxicity against HepG2 cells, with an IC_{50} of 60 μM.

In summary, only four multitarget compounds (**5**, **8**, **16** and **17**) with simultaneous activity towards H_3R and cholinesterases were obtained in the present work. All of them are propionyl phenoxy derivatives. Unfortunately, pharmacological studies have shown that these compounds have a much greater affinity for hH_3R (effects in the nanomolar range) than against cholinesterases (effects in the micromolar range).

In conclusion, among the series of compounds synthesized (**2**–**17**), azepane derivatives **16** and **17** proved to be the most promising ligands. Both of them can be used as lead compounds for further structural modifications. In particular, the change of length of the carbon linker (an elongation of greater than seven atoms) and/or an exchange of the ethyl substituent for a longer alkyl group (e.g., a butyl or a pentyl group) could be promising.

4. Materials and Methods

4.1. Synthesis of Compounds

Reagents and solvents were purchased from Merck and Alfa Aesar.

The course of the reaction was controlled using TLC (Merck silica 60F aluminum sheets; solvent: methylene chloride or methylene chloride: methanol 9:1). Spots were visualized under a UV lamp and/or stained with Dragendorf's reagent. NMR spectra (^1H and ^{13}C) were obtained in DMSO-d_6 on the following instruments: (^1H) -Mercury 300 MHz PFG spectrometer (Varian, Palo Alto, CA, USA) and (^{13}C)—FTNMR 500 MHz spectrometer (Joel Ltd., Akishima, Tokyo, Japan). Chemical shifts (δ) are given in ppm with respect to the solvent signal. Data are reported as follows: multiplicity (br s, broad singlet; d, dublet; m, multiplet; q, quartet; s, singlet; t, triplet), coupling constants (J) in Hz, and the number of protons. The mass spectrum (LC-MS) was recorded on a Waters TQ detector mass spectrometer (Water Corporation, Milford, CT, USA). Retention times (t_R) are given in minutes. All compounds (except **6**, **11** and **17**) showed a purity of >95%. Elemental analysis was performed on an Elemental Analyser Vario El-III (Hanau, Germany). The results are in agreement with the theoretical values, within ±0.4%. Melting points (Mp) were determined on a MEL-TEMP melting point apparatus II (LD Inc., Long Beach, CA, USA), and are uncorrected.

4.1.1. Synthesis of Compounds **1a**–**1d**

Bromides **1a**–**1d** were synthesized as described previously by Łażewska et al. [33], from 1-(4-hydroxyphenyl)ethan-1-one or 1-(4-hydroxyphenyl)propan-1-one, and dibromopentane or dibromohexane, respectively. After preliminary purification, crude products were used for further synthesis:

1-(4-((5-bromopentyl)oxy)phenyl)ethan-1-one CAS 61270-21-1 (**1a**)
1-(4-((6-bromohexyl)oxy)phenyl)ethan-1-one CAS138107-19-4 (**1b**)
1-(4-((5-bromopentyl)oxy)phenyl)propan-1-one (**1c**)
1-(4-((6-bromohexyl)oxy)phenyl)propan-1-one(**1d**)

4.1.2. Synthesis of Compounds **2**–**17**

The compounds were obtained by reflux (12–20 h) of a proper bromide **1a**–**1d** with an amine in the mixture of ethanol:water (21:4), and in the presence of potassium carbonate and a catalytic amount of potassium iodide. The precise procedure is described in reference [33]. After purification, the oily products were transformed into salts of oxalic acid.

1-(4-((5-(Piperidin-1-yl)pentyl)oxy)phenyl)ethan-1-one hydrogen oxalate (**2**)

From 1-(4-((5-bromopentyl)oxy)phenyl)ethan-1-one (1.42 g, 5 mmol) and piperidine (0.85 g, 10 mmol). Yield 28%. Mp 117–120 °C. $C_{18}H_{27}NO_2 \times C_2H_2O_4$ (MW = 379.44). Anal. calcd. for $C_{20}H_{29}NO_6$: C, 63.30; H, 7.70; N, 3.69%. Found: C, 63.00; H, 7.57; N, 3.52%. LC-MS: purity 96.58% t_R = 3.72, (ESI) m/z $[M+H]^+$ 290.315. ^{1}H NMR (300 MHz, DMSO-d_6) δ: 7.90 (d, *J* = 8.72 Hz, 2H), 7.01 (d, *J* = 8.72 Hz, 2H), 4.05 (t, *J* = 6.28 Hz, 2H), 2.86–3.45 (m, 5H), 2.49 (s, 3H), 1.61–1.85 (m, 8H), 1.29–1.58 (m, 4H). ^{13}C NMR (126 MHz, DMSO-d_6) δ: 196.8, 165.4, 163.0, 131.0, 130.3, 114.8, 68.0, 56.2, 52.4, 28.5, 26.9, 23.4, 23.3, 23.0, 22.1.

1-(4-((6-(Piperidin-1-yl)hexyl)oxy)phenyl)ethan-1-one hydrogen oxalate (**3**)

From 1-(4-((6-bromohexyl)oxy)phenyl)ethan-1-one (1.50 g, 5 mmol) and piperidine (0.85 g, 10 mmol). Yield 42%. Mp 116–119 °C. $C_{19}H_{29}NO_2 \times C_2H_2O_4$ (MW = 393.47). Anal. calcd. for $C_{21}H_{31}NO_6$: C, 64.10; H, 7.94; N, 3.56%. Found: C, 64.16; H, 8.18; N, 3.40%. LC-MS: purity 100% t_R = 4.16, (ESI) m/z $[M+H]^+$ 304.329. ^{1}H NMR (300 MHz, DMSO-d_6) δ: 7.90 (d, *J* = 8.72 Hz, 2H), 7.00 (d, *J* = 8.98 Hz, 2H), 4.04 (t, *J* = 6.41 Hz, 2H), 2.83–3.38 (m, 6H), 2.49 (s, 3H), 1.58–1.78 (m, 8H), 1.21–1.54 (m, 6H). ^{13}C NMR (126 MHz, DMSO-d_6) δ: 196.8, 165.4, 163.1, 131.0, 130.3, 114.8, 68.2, 56.3, 52.4, 28.8, 26.9, 26.4, 25.5, 23.6, 23.0, 22.0.

1-(4-((5-(Piperidin-1-yl)pentyl)oxy)phenyl)propan-1-one hydrogen oxalate (**4**)

From 1-(4-((5-bromopentyl)oxy)phenyl)propan-1-one (1.50 g, 5 mmol) and 4-methylpiperidine (0.99 g, 10 mmol). Yield 41%. Mp 130–132 °C. $C_{19}H_{29}NO_2 \times C_2H_2O_4$ (MW = 393.47). Anal. calcd. for $C_{21}H_{31}NO_6$: C, 64.10; H, 7.94; N, 3.56%. Found: C, 64.34; H, 8.18; N, 3.54%. LC-MS: purity 100% t_R = 4.38, (ESI) m/z $[M+H]^+$ 304.332. ^{1}H NMR (300 MHz, DMSO-d_6) δ: 7.91 (d, *J* = 8.72 Hz, 2H), 7.00 (d, *J* = 8.72 Hz, 2H), 4.04 (t, *J* = 6.28 Hz, 2H), 2.80–3.40 (m, 8H), 1.60–1.80 (m, 8H), 1.30–1.60 (m, 4H), 1.05 (t, *J* = 7.18 Hz, 3H). ^{13}C NMR (126 MHz, DMSO-d_6) δ 199.3, 165.4, 162.9, 130.6, 130.0, 114.9, 68.0, 56.2, 52.4, 31.3, 28.5, 23.4, 23.3, 23.0, 22.1, 8.8.

1-(4-((6-(Piperidin-1-yl)hexyl)oxy)phenyl)propan-1-one hydrogen oxalate (**5**)

From 1-(4-((6-bromohexyl)oxy)phenyl)propan-1-one (1.57 g, 5 mmol) and piperidine (0.85 g, 10 mmol). Yield 44%. Mp 120–122 °C. $C_{20}H_{31}NO_2 \times C_2H_2O_4$ (MW = 407.49). Anal. calcd. for $C_{22}H_{33}NO_6$: C, 64.84; H, 8.16; N, 3.44%. Found: C, 64.91; H, 8.13; N, 3.53%. LC-MS: purity 100% t_R = 4.75, (ESI) m/z $[M+H]^+$ 318.353. ^{1}H NMR (300 MHz, DMSO-d_6) δ: 7.91 (d, *J* = 8.72 Hz, 2H), 7.00 (d, *J* = 8.72 Hz, 2H), 4.03 (t, *J* = 6.41 Hz, 2H), 2.81–3.38 (m, 8H), 1.22–1.86 (m, 14H), 1.04 (t, *J* = 7.18 Hz, 3H). ^{13}C NMR (126 MHz, DMSO-d_6) δ: 199.3, 165.4, 162.9, 130.6, 129.9, 114.8, 68.2, 56.3, 52.4, 31.3, 26.4, 25.5, 23.0, 22.0, 8.8.

1-(4-((5-(3-Methylpiperidin-1-yl)pentyl)oxy)phenyl)ethan-1-one hydrogen oxalate (**6**)

From 1-(4-((5-bromopentyl)oxy)phenyl)ethan-1-one (1.42 g, 5 mmol) and 3-methylpiperidine (0.99 g, 10 mmol). Yield 33%. Mp 117–120 °C. $C_{19}H_{29}NO_2 \times C_2H_2O_4$ (MW = 393.47). Anal. calcd. for $C_{21}H_{31}NO_6$: C, 64.10; H, 7.94; N, 3.56%. Found: C, 64.15; H, 7.96; N, 3.31%. LC-MS: purity 92.42% t_R = 4.11, (ESI) m/z $[M+H]^+$ 304.340. ^{1}H NMR (300 MHz, DMSO-d_6) δ: 7.90 (d, *J* = 8.98 Hz, 2H), 7.01 (d, *J* = 8.98 Hz, 2H), 4.05 (t, *J* = 6.16 Hz, 2H), 3.23–3.43 (m, 2H), 2.88–3.03 (m, 2H), 2.69 (br. s., 1H), 2.49 (s, 3H), 2.33–2.46 (m, 1H), 1.54–1.90 (m, 8H), 1.33–1.50 (m, 2H), 1.04 (d, *J* = 11.54 Hz, 1H), 0.78–0.92 (m, 3H). ^{13}C NMR (126 MHz, DMSO-d_6) δ: 196.8, 165.4, 163.0, 131.0, 130.3, 114.8, 68.0, 57.9, 56.3, 56.2, 51.9, 30.6, 28.5, 26.9, 23.4, 23.3, 19.1.

1-(4-((6-(3-Methylpiperidin-1-yl)hexyl)oxy)phenyl)ethan-1-one hydrogen oxalate (**7**)

From 1-(4-((6-bromohexyl)oxy)phenyl)ethan-1-one (1.50 g, 5 mmol) and 3-methylpiperidine (0.99 g, 10 mmol). Yield 39%. Mp 90–93 °C. $C_{20}H_{31}NO_2 \times C_2H_2O_4$ (MW = 407.47). Anal. calcd. for $C_{22}H_{33}NO_6$: C, 64.84; H, 8.16; N, 3.44%. Found: C, 64.58; H, 8.29; N, 3.34%. LC-MS: purity 100% t_R = 4.53, (ESI) m/z $[M+H]^+$ 318.350. ^{1}H NMR (300 MHz, DMSO-d_6) δ: 7.90 (d, *J* = 8.98 Hz, 2H), 7.00 (d, *J* = 8.98 Hz, 2H), 4.04 (t, *J* = 6.28 Hz, 2H), 3.31 (t, *J* = 14.11 Hz, 2H), 2.83–3.03 (m, 2H), 2.68 (br. s., 1H), 2.49 (s, 3H), 2.31–2.45 (m, 1H), 1.54–1.96 (m, 8H), 1.22–1.51 (m, 4H), 0.93–1.12 (m, 1H), 0.86 (d, *J* = 6.67 Hz, 3H). ^{13}C NMR (126 MHz, DMSO-d_6) δ: 196.8, 165.3, 163.1, 131.0, 130.3, 114.8, 68.2, 57.9, 56.3, 51.9, 30.6, 28.8, 26.9, 26.4, 25.5, 23.6, 22.5, 19.1.

1-(4-((5-(3-Methylpiperidin-1-yl)pentyl)oxy)phenyl)propan-1-one hydrogen oxalate (**8**)

From 1-(4-((5-bromopentyl)oxy)phenyl)propan-1-one (1.5 g, 5 mmol) and 3-methylpiperidine (0.99 g, 10 mmol). Yield 42%. Mp 132–134 °C. $C_{20}H_{31}NO_2 \times C_2H_2O_4$ (MW = 407.49). Anal. calcd. for $C_{22}H_{33}NO_6$: C, 64.84; H, 8.16; N, 3.44%. Found: C, 64.80; H, 8.43; N, 3.54%. LC-MS: purity 100% t_R = 4.74, (ESI) m/z $[M+H]^+$ 318.349. ^{1}H NMR (300 MHz, DMSO-d_6) δ: 7.91 (d, *J* = 8.72 Hz, 2H), 7.00 (d, *J* = 8.72 Hz, 2H), 4.04 (t, *J* = 6.28 Hz, 2H), 3.21–3.42 (m, 2H), 2.86–3.07 (m, 4H), 2.60–2.78 (m, 1H), 2.34–2.45 (m, 1H), 1.53–1.97 (m, 8H), 1.31–1.52 (m, 2H), 1.05 (t, *J* = 7.18 Hz, 4H), 0.86 (d, *J* = 6.41 Hz, 3H). ^{13}C NMR (126 MHz, DMSO-d_6) δ: 199.33, 165.34, 162.87, 130.62, 129.97, 114.78, 68.0, 57.88, 56.27, 51.93, 31.30, 30.62, 28.95, 28.52, 23.40, 23.26, 22.69, 19.13, 8.84.

1-(4-((6-(3-Methylpiperidin-1-yl)hexyl)oxy)phenyl)propan-1-one hydrogen oxalate (**9**)

From 1-(4-((6-bromohexyl)oxy)phenyl)propan-1-one (1.57 g, 5 mmol) and 3-methylpiperidine (0.99 g, 10 mmol). Yield 36%. Mp 77–80 °C. $C_{21}H_{33}NO_2 \times C_2H_2O_4$ (MW = 421.52). Anal. calcd. for $C_{23}H_{35}NO_6$: C, 65.53; H, 8.37; N, 3.32%. Found: C, 65.68; H, 8.35; N, 3.43%. LC-MS: purity 100% t_R = 5.07, (ESI) m/z $[M+H]^+$ 332.382. ^{1}H NMR (300 MHz, DMSO-d_6) δ: 7.91 (d, *J* = 8.98 Hz, 2H), 7.00 (d, *J* = 8.98 Hz, 2H), 4.03 (t, *J* = 6.28 Hz, 2H), 3.21–3.41 (m, 2H), 2.82–3.03 (m, 4H), 2.68 (t, *J* = 10.39 Hz, 1H), 2.34–2.45 (m, 1H), 1.54–1.92 (m, 8H), 1.19–1.51 (m, 4H), 1.04 (t, *J* = 7.18 Hz, 4H), 0.86 (d, *J* = 6.41 Hz, 3H). ^{13}C NMR (126 MHz, DMSO-d_6) δ: 199.3, 165.3, 162.9, 130.6, 129.9, 114.8, 68.2, 57.9, 56.4, 51.9, 31.3, 30.6, 29.0, 28.8, 26.4, 25.5, 23.6, 22.7, 19.1, 8.8.

1-(4-((5-(4-Methylpiperidin-1-yl)pentyl)oxy)phenyl)ethan-1-one hydrogen oxalate (**10**)

From 1-(4-((5-bromopentyl)oxy)phenyl)ethan-1-one (1.42 g, 5 mmol) and 4-methylpiperidine (0.99 g, 10 mmol). Yield 32%. Mp 122–125 °C. $C_{19}H_{29}NO_2$ x $C_2H_2O_4$ (MW = 393.47). Anal. calcd. for $C_{21}H_{31}NO_6$: C, 64.10; H, 7.94; N, 3.56%. Found: C, 63.75; H, 7.85; N, 3.54%. LC-MS: purity 100% t_R = 4.12 (ESI) m/z $[M+H]^+$ 304.332. ^{1}H NMR (300 MHz, DMSO-d_6) δ: 7.90 (d, *J* = 8.72 Hz, 2H), 7.01 (d, *J* = 8.72 Hz, 2H), 4.05 (t, *J* = 6.28 Hz, 2H), 3.28–3.46 (m, 2H), 2.90–3.05 (m, 2H), 2.81 (t, *J* = 11.41 Hz, 2H), 2.49 (s, 3H), 1.51–1.83 (m, 7H), 1.21–1.48 (m, 4H), 0.90 (d, *J* = 6.41 Hz, 3H). ^{13}C NMR (126 MHz, DMSO-d6) δ: 196.80, 165.34, 163.01, 131.02, 130.32, 114.77, 68.03, 55.94, 51.87, 30.99, 28.50, 26.93, 23.53, 23.25, 21.38.

1-(4-((6-(4-Methylpiperidin-1-yl)hexyl)oxy)phenyl)ethan-1-one hydrogen oxalate (**11**)

From 1-(4-((6-bromohexyl)oxy)phenyl)ethan-1-one (1.50 g, 5 mmol) and 4-methylpiperidine (0.99 g, 10 mmol). Yield 48%. Mp 111–114 °C. $C_{20}H_{31}NO_2 \times C_2H_2O_4$ (MW = 407.47). Anal. calcd. for $C_{22}H_{33}NO_6$: C, 64.84; H, 8.16; N, 3.44%. Found: C, 65.79; H, 8.70; N, 3.22%. LC-MS: purity 94.57% t_R = 4.45, (ESI) m/z $[M+H]^+$ 318.359. ^{1}H NMR (300 MHz, DMSO-d_6) δ: 7.90 (d, *J* = 8.72 Hz, 2H), 7.00 (d, *J* = 8.72 Hz, 2H), 4.04 (t, *J* = 6.28 Hz, 2H), 3.24–3.46 (m, 2H), 2.68–3.03 (m, 4H), 2.49 (s, 3H), 1.20–1.85 (m, 13H), 0.90 (d, *J* = 6.41 Hz, 3H). ^{13}C NMR (126 MHz, DMSO-d_6) δ: 196.8, 165.3, 163.1, 131.0, 130.3, 114.8, 68.2, 28.8, 26.9, 26.4, 25.5, 23.7.

1-(4-((5-(4-Methylpiperidin-1-yl)pentyl)oxy)phenyl)propan-1-one hydrogen oxalate (**12**)

From 1-(4-((5-bromopentyl)oxy)phenyl)propan-1-one (1.50 g, 5 mmol) and 4-methylpiperidine (0.99 g, 10 mmol). Yield 39%. Mp 142–145 °C. $C_{20}H_{31}NO_2 \times C_2H_2O_4$ (MW = 407.49). Anal. calcd. for $C_{22}H_{33}NO_6$: C, 64.84; H, 8.16; N, 3.44%. Found: C, 64.97; H, 8.48; N, 3.49%. LC-MS: purity 98.17% t_R = 4.54, (ESI) m/z $[M+H]^+$ 318.366. ^{1}H NMR (300 MHz, DMSO-d_6) δ: 7.90 (d, *J* = 8.72 Hz, 2H), 7.00 (d, *J* = 8.72 Hz, 2H), 4.04 (t, *J* = 6.28 Hz, 2H), 3.35 (d, *J* = 11.54 Hz, 2H), 2.95 (q, *J* = 7.18 Hz, 4H), 2.81 (t, *J* = 11.54 Hz, 2H), 1.51–1.88 (m, 7H),

1.27–1.49 (m, 4H), 1.04 (t, *J* = 7.18 Hz, 3H), 0.83–0.94 (m, 3H). ^{13}C NMR (126 MHz, DMSO-d_6) δ: 199.3, 165.4, 162.9, 130.6, 130.0, 114.8, 68.0, 55.9, 51.9, 31.3, 31.0, 28.5, 23.5, 23.3, 21.4, 8.8.

1-(4-((6-(4-Methylpiperidin-1-yl)hexyl)oxy)phenyl)propan-1-one hydrogen oxalate (**13**)

From 1-(4-((6-bromohexyl)oxy)phenyl)propan-1-one (1.57 g, 5 mmol) and 4-methylpiperidine (0.99 g, 10 mmol). Yield 38%. Mp 115–117 °C. $C_{21}H_{33}NO_2 \times C_2H_2O_4$ (MW = 421.52). Anal. calcd. for $C_{23}H_{35}NO_6$: C, 65.53; H, 8.37; N, 3.32%. Found: C, 65.59; H, 8.29; N, 3.41%. LC-MS: purity 100% t_R = 5.12, (ESI) m/z $[M+H]^+$ 332.372. ^{1}H NMR (300 MHz, DMSO-d_6) δ: 7.91 (d, *J* = 8.72 Hz, 2H), 7.00 (d, *J* = 8.72 Hz, 2H), 4.03 (t, *J* = 6.28 Hz, 2H), 3.23–3.47 (m, 2H), 2.87–3.04 (m, 4H), 2.80 (t, *J* = 11.54 Hz, 2H), 1.48–1.86 (m, 7H), 1.16–1.45 (m, 6H), 1.04 (t, *J* = 7.18 Hz, 3H), 0.71–0.93 (m, 3H). ^{13}C NMR (126 MHz, DMSO-d_6) δ: 199.3, 165.3, 162.9, 130.6, 129.9, 114.8, 68.2, 56.0, 51.9, 31.3, 31.0, 28.8, 28.5, 26.4, 25.5, 23.7, 21.4, 8.8.

1-(4-((5-(Azepan-1-yl)pentyl)oxy)phenyl)ethan-1-one hydrogen oxalate (**14**)

From 1-(4-((5-bromopentyl)oxy)phenyl)ethan-1-one (1.42 g, 5 mmol) and azepane (0.99 g, 10 mmol). Yield 24%. Mp 102–105 °C. $C_{19}H_{29}NO_2 \times C_2H_2O_4$ (MW = 393.47). Anal. calcd. for $C_{21}H_{31}NO_6$: C, 64.10; H, 7.94; N, 3.56%. Found: C, 63.77; H, 7.94; N, 3.57%. LC-MS: purity 97.81% t_R = 4.04, (ESI) m/z $[M+H]^+$ 304.336. ^{1}H NMR (300 MHz, DMSO-d_6) δ: 7.90 (d, *J* = 8.72 Hz, 2H), 7.01 (d, *J* = 8.72 Hz, 2H), 4.05 (t, *J* = 6.28 Hz, 2H), 3.18 (br. s., 4H), 2.94–3.08 (m, 2H), 2.49 (s, 3H), 1.51–1.86 (m, 12H), 1.32–1.49 (m, 2H). ^{13}C NMR (126 MHz, DMSO-d_6) δ 196.8, 165.4, 163.0, 131.0, 130.3, 114.8, 68.1, 56.6, 54.0, 28.5, 26.9, 26.6, 23.8, 23.5, 23.3.

1-(4-((6-(Azepan-1-yl)hexyl)oxy)phenyl)ethan-1-one hydrogen oxalate (**15**)

From 1-(4-((6-bromohexyl)oxy)phenyl)ethan-1-one (1.50 g, 5 mmol) and azepane (0.99 g, 10 mmol). Yield 38%. Mp 91–94 °C. $C_{20}H_{31}NO_2 \times C_2H_2O_4$ (MW = 407.47). Anal. calcd. for $C_{22}H_{33}NO_6$: C, 64.84; H, 8.16; N, 3.44%. Found: C, 64.75; H, 8.36; N, 3.28%. LC-MS: purity 100% t_R = 4.46, (ESI) m/z $[M+H]^+$ 318.351. ^{1}H NMR (300 MHz, DMSO-d_6) δ:7.90 (d, *J* = 8.72 Hz, 2H), 7.00 (d, *J* = 8.72 Hz, 2H), 4.04 (t, *J* = 6.28 Hz, 2H), 3.16 (d, *J* = 4.36 Hz, 4H), 2.93–3.06 (m, 2H), 2.49 (s, 3H), 1.69–1.86 (m, 6H), 1.51–1.68 (m, 6H), 1.23–1.49 (m, 4H). ^{13}C NMR (126 MHz, DMSO-d_6) δ: 196.8, 165.4, 163.1, 131.0, 130.3, 114.8, 68.2, 56.7, 53.9, 28.8, 26.9, 26.6, 26.4, 25.5, 24.0, 23.5.

1-(4-((5-(Azepan-1-yl)pentyl)oxy)phenyl)propan-1-one hydrogen oxalate (**16**)

From 1-(4-((5-bromopentyl)oxy)phenyl)propan-1-one (1.50 g, 5 mmol) and azepane (0.99 g, 10 mmol). Yield 32%. Mp 132–134 °C. $C_{20}H_{31}NO_2 \times C_2H_2O_4$ (MW = 407.49). Anal. calcd. for $C_{22}H_{33}NO_6$: C, 64.84; H, 8.16; N, 3.44%. Found: C, 64.66; H, 8.33; N, 3.44%. LC-MS: purity 98.59% t_R = 4.68, (ESI) m/z $[M+H]^+$ 318.350. ^{1}H NMR (300 MHz, DMSO-d_6) δ: 7.91 (d, *J* = 8.72 Hz, 2H), 7.00 (d, *J* = 8.72 Hz, 2H), 4.05 (t, *J* = 6.41 Hz, 2H), 3.18 (br s., 4H), 2.87–3.08 (m, 4H), 1.63–1.85 (m, 8H), 1.58 (br. s., 4H), 1.32–1.49 (m, 2H), 1.05 (t, *J* = 7.18 Hz, 3H). ^{13}C NMR (126 MHz, DMSO-d_6) δ: 199.33, 165.41, 162.87, 130.62, 129.98, 114.78, 68.03, 56.60, 53.94, 31.30, 28.52, 26.64, 23.82, 23.46, 23.26, 8.84.

1-(4-((6-(Azepan-1-yl)hexyl)oxy)phenyl)propan-1-one hydrogen oxalate (**17**)

From 1-(4-((6-bromohexyl)oxy)phenyl)propan-1-one (1.57 g, 5 mmol) and azepane (0.99 g, 10 mmol). Yield 41%. Mp 98–100 °C. $C_{21}H_{33}NO_2 \times C_2H_2O_4$ (MW = 421.52). Anal. calcd. for $C_{23}H_{35}NO_6$: C, 65.53; H, 8.37; N, 3.32%. Found: C, 65.63; H, 8.54; N, 3.29%. LC-MS: purity 94.76% t_R = 5.11, (ESI) m/z $[M+H]^+$ 332.374. ^{1}H NMR (300 MHz, DMSO-d_6) δ: 7.91 (d, *J* = 8.72 Hz, 2H), 7.00 (d, *J* = 8.72 Hz, 2H), 4.03 (t, *J* = 6.41 Hz, 2H), 3.17 (br s, 4H), 2.86-3.05 (m, 4H), 1.49-1.87 (m, 12H), 1.20-1.46 (m, 4H), 1.04 (t, *J* = 7.18 Hz, 3H). ^{13}C NMR (126 MHz, DMSO-d_6) δ: 199.32, 165.40, 162.91, 130.62, 129.94, 114.76, 68.18, 56.69, 53.92, 31.30, 28.79, 26.63, 26.37, 25.52, 24.02, 23.45, 8.84.

4.2. Biological Studies

Compounds **2**–**17** were tested as oxalic acid salts.

4.2.1. Histamine H_3 Receptor Affinity

H_3R receptor affinity assays were performed in the radioligand competition assay. Human H_3R was stably expressed in HEK293 cells. [^{3}H]-N^{α}-Methylhistamine (K_D = 3.08 nM)

was used as the radioligand. The compounds used in the experiments were dissolved in DMSO. The precise experiment was performed as previously described [30]. Complete curves were obtained for at least seven approximate concentrations, in at least three independent experiments, performed at least in duplicate. K_i values were calculated using the Cheng–Prusoff equation. Results are presented as mean values with confidence intervals (CI) (95%).

4.2.2. Cholinesterase Inhibitory Activity

AChE from *electrophorus electricus* and BuChE from *equine serum* were purchased from Sigma-Aldrich (Steinheim, Germany). The whole procedure was performed as previously described, using a modified Ellman method in 96-well microplates [19]. Absorbance was measured using an EnSpire multimode microplate reader (PerkinElmer, Waltham, MA, USA) at 412 nm. Initial screening was performed for compounds at a concentration of 10 micromoles. The percentage of inhibition was calculated by comparison with a blank sample (100% enzyme activity). For compounds showing >70% inhibition of enzyme activity, IC_{50} values were determined, measuring absorbance at six different inhibitor concentrations. Each concentration was measured in triplicate. IC_{50} values were calculated using GrapPad Prism 9 software (GraphPad Software, San Diego, CA, USA). Data are expressed as mean ± SEM.

4.2.3. Kinetic Studies of Cholinesterases

Studies were performed with compounds **16** and **17** using a method as described previously [19]. Vmax and Km values of the Michaelis–Menten kinetics were calculated by nonlinear regression from substrate–velocity curves. Lineweaver–Burk and Cornish–Bowden plots were calculated using linear regression in GraphPad Prism 9 software (GraphPad Software, San Diego, CA, USA). Each experiment was performed in triplicate.

4.2.4. Monoamine Oxidase B Inhibitory Activity

The compounds were evaluated by the spectrophotometric method described earlier [2032]. The enzyme was purchased from Sigma-Aldrich (Steinheim, Germany). Screening was carried out at a concentration of 1 micromolar. Inhibitor activity was measured in the presence of p-tyramine. The percentage inhibition of reference compounds, pargiline and rasagiline, tested at 1 micromolar, were 95 and 100%, respectively.

Data are expressed as mean values of two independent experiments.

4.2.5. Toxicity Evaluation

The hepatoma cell line HepG2 (ATCC® HB-8065TM) and SH-SY5Y CRL-2266 neuroblastoma cell line were used to evaluate the toxicity of tested compounds. Tests were conducted as described previously [33]. The CellTiter 96® Aqueous Non-Radioactive Cell Proliferation Assay was purchased from Promega (Madison, WI, USA). Compounds were tested at 7 concentrations (0.78, 1.56, 3.125, 6.25, 12.5, 25 and 50 μM). Cell viability was determined after incubation with compounds for 72 h. Each experiment was performed twice, in triplicate.

Supplementary Materials: The following supporting information can be downloaded at: https://www.mdpi.com/article/10.3390/molecules28052349/s1, Spectral information (^{1}H-NMR and ^{13}C-NMR) of synthesized compounds and Figures S1 and S2 (toxicity evaluation in HepG2 and SH-SY5Y cells).

Author Contributions: Conceptualization, D.Ł. and K.K.-K.; synthesis of compounds, M.K. and K.K.-K.; in vitro histamine H_3R affinity studies: M.D. and H.S.; in vitro AChE and BuChE studies: P.Z., J.G. and A.W.; in vitro hMAO B studies: A.D.-P.; toxicity studies, E.H.-O.; original draft preparation: D.Ł.; critical revision of the manuscript: all authors; project administration: D.Ł. All authors have read and agreed to the published version of the manuscript.

Funding: This research was funded by Jagiellonian University Medical College in Kraków grant no N42/DBS/000300 (D.Ł.). M.D. and H.S. participate in the DFG funded GRK2158.

Institutional Review Board Statement: Not applicable.

Informed Consent Statement: Not applicable.

Data Availability Statement: Not applicable.

Acknowledgments: M.D. and H.S. kindly thank J.C. Schwartz (Bioprojet, Paris, France) for providing HEK293-hH_3R cells. M.D. and H.S. would like to thank for support the DFG (GRK2158).

Conflicts of Interest: The authors declare no conflict of interest.

Sample Availability: Samples of the compounds could be available from the authors.

References

1. Samanta, S.; Ramesh, M.; Govindaraju, T. Chapter 1: Alzheimer's is a Multifactorial Disease. In *Alzheimer's Disease: Recent Findings in Pathophysiology, Diagnostic and Therapeutic Modalities*, 1st ed.; RCS: London, UK, 2022; pp. 1–34. [CrossRef]
2. Knopman, D.S.; Amieva, H.; Petersen, R.C.; Chételat, G.; Holtzman, D.M.; Hyman, B.T.; Nixon, R.A.; Jones, D.T. Alzheimer disease. *Nat. Rev. Dis. Primers* **2021**, *7*, 33. [CrossRef]
3. Twohig, D.; Nielsen, H.M. α-synuclein in the pathophysiology of Alzheimer's disease. *Mol. Neurodegener.* **2019**, *14*, 23. [CrossRef] [PubMed]
4. Craig, L.A.; Hong, N.S.; McDonald, R.J. Revisiting the cholinergic hypothesis in the development of Alzheimer's disease. *Neurosci. Biobehav. Rev.* **2011**, *35*, 1397–1409. [CrossRef] [PubMed]
5. Zhang, H.; Wang, Y.; Wang, Y.; Li, X.; Wang, S.; Wang, Z. Recent advance on carbamate-based cholinesterase inhibitors as potential multifunctional agents against Alzheimer's disease. *Eur. J. Med. Chem.* **2022**, *240*, 114606. [CrossRef]
6. Pardo-Moreno, T.; González-Acedo, A.; Rivas-Domínguez, A.; García-Morales, V.; García-Cozar, F.J.; Ramos-Rodríguez, J.J.; Melguizo-Rodríguez, L. Therapeutic Approach to Alzheimer's Disease: Current Treatments and New Perspectives. *Pharmaceutics* **2022**, *14*, 1117. [CrossRef] [PubMed]
7. Vecchio, I.; Sorrentino, L.; Paoletti, A.; Marra, R.; Arbitrio, M. The State of The Art on Acetylcholinesterase Inhibitors in the Treatment of Alzheimer's Disease. *J. Cent. Nerv. Syst. Dis.* **2021**, *13*, 11795735211029113. [CrossRef] [PubMed]
8. Cheong, S.L.; Tiew, J.K.; Fong, Y.H.; Leong, H.W.; Chan, Y.M.; Chan, Z.L.; Kong, E.W.J. Current Pharmacotherapy and Multi-Target Approaches for Alzheimer's Disease. *Pharmaceuticals* **2022**, *15*, 1560. [CrossRef]
9. Lopes, F.B.; Aranha, C.M.S.Q.; Fernandes, J.P.S. Histamine H_3 receptor and cholinesterases as synergistic targets for cognitive decline: Strategies to the rational design of multitarget ligands. *Chem. Biol. Drug Des.* **2021**, *98*, 212–225. [CrossRef] [PubMed]
10. Arrang, J.M.; Garbarg, M.; Schwartz, J.C. Auto-inhibition of brain histamine release mediated by a novel class (H3) of histamine receptor. *Nature* **1983**, *302*, 832–837. [CrossRef]
11. Panula, P.; Chazot, P.L.; Cowart, M.; Gutzmer, R.; Leurs, R.; Liu, W.L.; Stark, H.; Thurmond, R.L.; Haas, H.L. International Union of Basic and Clinical Pharmacology. XCVIII. Histamine receptors. *Pharmacol. Rev.* **2015**, *67*, 601–655. [CrossRef]
12. Nieto-Allamila, G.; Márquez-Gómez, R.; García-Gálvez, A.M.; Morales-Figueroa, G.E.; Arias-Montaño, J.A. The Histamine H_3 Receptor: Structure, pharmacology, and Function. *Mol. Pharmacol.* **2016**, *90*, 649–673. [CrossRef]
13. Ghamari, N.; Zarei, O.; Arias-Montaño, J.A.; Reiner, D.; Dastmalchi, S.; Stark, H.; Hamzeh-Mivehroud, M. Histamine H_3 receptor antagonists/inverse agonists: Where do they go? *Pharmacol. Ther.* **2019**, *200*, 69–84. [CrossRef]
14. Łażewska, D.; Kieć-Kononowicz, K. Progress in the development of histamine H_3 receptor antagonists/inverse agonists: A patent review (2013–2017). *Expert Opin. Ther. Pat.* **2018**, *28*, 175–196. [CrossRef]
15. Kubo, M.; Kishi, T.; Matsunaga, S.; Iwata, N. Histamine H_3 receptor antagonists for Alzheimer's Disease: A Systematic Review and Meta-Analysis of Randomized Placebo-Controlled Trials. *J. Alzheimers Dis.* **2015**, *48*, 667–671. [CrossRef] [PubMed]
16. Peng, X.; Yang, L.; Liu, Z.; Lou, S.; Mei, S.; Li, M.; Chen, Z.; Zhang, H. Structural basis for recognition of antihistamine drug by human histamine receptor. *Nat. Commun.* **2022**, *13*, 6105. [CrossRef] [PubMed]
17. Ghamari, N.; Dastmalchi, S.; Zarei, O.; Arias-Montaño, J.A.; Reiner, D.; Ustun-Alkan, F.; Stark, H.; Hamzeh-Mivehroud, M. In silico and in vitro studies of two non-imidazole multiple targeting agents at histamine H_3 receptors and cholinesterase enzymes. *Chem. Biol. Drug Des.* **2020**, *95*, 279–290. [CrossRef] [PubMed]
18. Wang, D.; Hu, M.; Li, X.; Zhang, D.; Chen, C.; Fu, J.; Shao, S.; Shi, G.; Zhou, Y.; Wu, S.; et al. Design, synthesis, and evaluation of isoflavone analogs as multifunctional agents for the treatment of Alzheimer's disease. *Eur. J. Med. Chem.* **2019**, *168*, 207–220. [CrossRef]
19. Bajda, M.; Łażewska, D.; Godyń, J.; Zaręba, P.; Kuder, K.; Hagenow, S.; Łątka, K.; Stawarska, E.; Stark, H.; Kieć-Kononowicz, K.; et al. Search for new multi-target compounds against Alzheimer's disease among histamine H_3 receptor ligands. *Eur. J. Med. Chem.* **2020**, *185*, 111785. [CrossRef] [PubMed]
20. Łażewska, D.; Bajda, M.; Kaleta, M.; Zaręba, P.; Doroz-Płonka, A.; Siwek, A.; Alachkar, A.; Mogilski, S.; Saad, A.; Kuder, K.; et al. Rational design of new multitarget histamine H_3 receptor ligands as potential candidates for treatment of Alzheimer's disease. *Eur. J. Med. Chem.* **2020**, *207*, 112743. [CrossRef]

21. Godyń, J.; Zaręba, P.; Łażewska, D.; Stary, D.; Reiner-Link, D.; Frank, A.; Latacz, G.; Mogilski, S.; Kaleta, M.; Doroz-Płonka, A.; et al. Cyanobiphenyls: Novel H_3 receptor ligands with cholinesterase and MAO B inhibitory activity as multitarget compounds for potential treatment of Alzheimer's disease. *Bioorg. Chem.* **2021**, *14*, 105129. [CrossRef]
22. Lopes, F.B.; Aranha, C.M.S.Q.; Corrêa, M.F.; Fernandes, G.A.B.; Okamoto, D.N.; Simões, L.P.M.; Junior, N.M.N.; Fernandes, J.P.S. Evaluation of the histamine H_3 receptor antagonists from LINS01 series as cholinesterases inhibitors: Enzymatic and modeling studies. *Chem. Biol. Drug Des.* **2022**, *100*, 722–729. [CrossRef]
23. Finberg, J.P.M. Inhibitors of MAO-B and COMT: Their Effects on Brain Dopamine Levels and Uses in Parkinson's Disease. *J. Neural. Transm.* **2019**, *126*, 433–448. [CrossRef] [PubMed]
24. Pan, X.; Kaminga, A.C.; Wen, S.W.; Wu, X.; Acheampong, K.; Liu, A. Dopamine and Dopamine Receptors in Alzheimer's Disease: A Systematic Review and Network Meta-Analysis. *Front. Aging Neurosci.* **2019**, *11*, 175. [CrossRef] [PubMed]
25. Nam, E.; Derrick, J.S.; Lee, S.; Kang, J.; Han, J.; Lee, S.J.C.; Chung, S.W.; Lim, M.H. Regulatory Activities of Dopamine and Its Derivatives toward Metal-Free and Metal-Induced Amyloid-β Aggregation, Oxidative Stress, and Inflammation in Alzheimer's Disease. *ACS Chem. Neurosci.* **2018**, *9*, 2655–2666. [CrossRef]
26. Godyń, J.; Zaręba, P.; Stary, D.; Kaleta, M.; Kuder, K.J.; Latacz, G.; Mogilski, S.; Reiner-Link, D.; Frank, A.; Doroz-Płonka, A.; et al. Benzophenone Derivatives with Histamine H_3 Receptor Affinity and Cholinesterase Inhibitory Potency as Multitarget-Directed Ligands for Possible Therapy of Alzheimer's Disease. *Molecules* **2023**, *28*, 238. [CrossRef] [PubMed]
27. Sadek, B.; Łażewska, D.; Hagenow, S.; Kieć-Kononowicz, K.; Stark, H. Histamine H_3R Antagonists: From Scaffold Hopping to Clinical Candidates. In *Histamine Receptors. Preclinical and Clinical Aspects*; Blandina, P., Passani, M., Eds.; Springer International Publishing: Cham, Switzerland, 2016; pp. 109–155. [CrossRef]
28. Chmiel, T.; Mieszkowska, A.; Kempińska-Kupczyk, D.; Kot-Wasik, A.; Namieśnik, J.; Mazerska, Z. The impact of lipophilicity on environmental processes, drug delivery and bioavailability of food components. *Microchem. J.* **2019**, *146*, 393–406. [CrossRef]
29. Available online: http://www.swissadme.ch/ (accessed on 28 December 2022).
30. Kottke, T.; Sander, K.; Weizel, L.; Schneider, E.H.; Seifert, R.; Stark, H. Receptor-specific functional efficacies of alkyl imidazoles as dual histamine H3/H4 receptor ligands. *Eur. J. Pharmacol.* **2011**, *654*, 200–208. [CrossRef]
31. Ellman, G.L.; Courtney, K.D.; Anders, V., Jr.; Feather-Stone, R.M. A new and rapid colorimetric determination of acetylcholinesterase activity. *Biochem. Pharmacol.* **1961**, *7*, 88–95. [CrossRef]
32. Łażewska, D.; Olejarz-Maciej, A.; Kaleta, M.; Bajda, M.; Siwek, A.; Karcz, T.; Doroz-Płonka, A.; Cichoń, U.; Kuder, K.; Kieć-Kononowicz, K. 4-tert-Pentylphenoxyalkyl derivatives–Histamine H_3 receptor ligands and monoamine oxidase B inhibitors. *Bioorg. Med. Chem. Lett.* **2018**, *28*, 3596–3600. [CrossRef]
33. Łażewska, D.; Kaleta, M.; Schwed, J.S.; Karcz, T.; Mogilski, S.; Latacz, G.; Olejarz, A.; Siwek, A.; Kubacka, M.; Lubelska, A.; et al. Biphenyloxy-alkyl-piperidine and azepane derivatives as histamine H_3 receptor ligands. *Bioorg. Med. Chem.* **2017**, *25*, 5341–5354. [CrossRef]
34. Ramirez, T.; Strigun, A.; Verlohner, A.; Huener, H.A.; Peter, E.; Herold, M.; Bordag, N.; Mellert, W.; Walk, T.; Spitzer, M.; et al. Prediction of liver toxicity and mode of action using metabolomics in vitro in HepG2 cells. *Arch Toxicol.* **2018**, *92*, 893–906. [CrossRef] [PubMed]
35. Bell, M.; Zempel, H. SH-SY5Y-derived neurons: A human neuronal model system for investigating TAU sorting and neuronal subtype-specific TAU vulnerability. *Rev. Neurosci.* **2021**, *33*, 1–15. [CrossRef] [PubMed]

Disclaimer/Publisher's Note: The statements, opinions and data contained in all publications are solely those of the individual author(s) and contributor(s) and not of MDPI and/or the editor(s). MDPI and/or the editor(s) disclaim responsibility for any injury to people or property resulting from any ideas, methods, instructions or products referred to in the content.